

## A Method for the Measurement of the True Die Swell of Polymer Melts

L. A. UTRACKI,\* Z. BAKERDJIAN, and MUSA R. KAMAL,  
*Department of Chemical Engineering, McGill University, Montreal, Canada*

### Synopsis

A new device has been designed for the measurement of the die swell of extruded polymer melts. According to the proposed procedure, samples can be collected, annealed, and photographed. The device may be used in conjunction with any capillary-type rheometer. It can accommodate simultaneously as many samples as it is needed. The samples are suspended in a thermostated liquid, carefully selected for each polymer. The liquids must be thermally stable and of proper density and thermodynamic and interfacial properties. The device was used in conjunction with the Instron capillary rheometer, ICR. Three types of polymer were tested: polystyrene (PS), polyethylene (PE), and a semirigid poly(vinyl chloride) formulation (PVC). The swelling of the extrudates was followed for ca. 40 min; the equilibrium dimensions were usually reached within the first 2 min. Parallel with these measurements, the samples were tested in the Weissenberg rheogoniometer (WR) recording both shear and normal stresses. For PS and PE, the flow curves determined in these two rheometers overlapped, while they differed for PVC. The swell ratio,  $B_{exp} = D/D_0$  (where  $D$  and  $D_0$  are the equilibrium diameter of the extrudate and diameter of the capillary, respectively), was converted to recoverable shear strain,  $s$ , as follows. First,  $B_{exp}$  and  $s$  were determined in ICR and WR, respectively, for a PS sample over wide and overlapping ranges of rate of shear. This experimental dependence was found to follow Tanner's theoretical relation. Consequently, this relation was used to compute  $s$  from  $B_{exp}$  for all the other samples. Excellent agreement was observed between the  $s$  values calculated from  $B_{exp}$  and  $s$  values determined in WR.

### INTRODUCTION

Extrudate swelling is observed when a polymer melt emerges from a bounded channel into another larger or open channel or into the atmosphere. The phenomenon is called die swell (DS), Barrus effect, memory swelling, puff up, etc. In this paper, the first term will be used.

The main goal of this work was to develop a fast, inexpensive, and precise method for measuring the true die swell of polymer melts. Therefore, it was necessary to provide conditions under which the swelling would occur isothermally, on completely relaxed samples in the absence of gravitational sagging and interfacial tension effects. In order to maintain isothermal conditions, it was desirable to collect the samples in a thermostating chamber, just below the exit of the capillary.

\* Currently with Explosives Research Laboratory, Canadian Industries Ltd., McMasterville, Quebec, Canada J3G 1T9.

The second goal of this project was to correlate the experimental  $DS = f(\text{rate of shear, } \dot{\gamma})$  dependence with the material parameters of the sample. For this reason, several theoretical, semitheoretical, and empirical relations between  $DS$  and the recoverable shear strain  $s$  were compared with the experimental results. On the basis of this comparison, suitable correlations would be sought to calculate the primary normal stress difference from  $DS$ .

### THEORETICAL

In capillary flow, a measure of  $DS$  is the ratio of extrudate to capillary diameters:

$$B_{\text{exp}} = D/D_0. \quad (1)$$

Experimentally,  $D$  should be measured on a completely relaxed strand, extruded through an infinitely long capillary to a medium at the same temperature as that of the extruding device. In practice, the material is extruded through a sufficiently long capillary to provide nearly the equilibrium dimension of the strand, and is either quenched and subsequently reheated or is allowed to relax at a temperature which is usually lower than the extrusion temperature.

Most of the theoretical or semitheoretical relations propose to correlate  $B_{\text{exp}}$  with the recoverable shear strain, defined from Hooke's law as

$$s = J_e^0 \sigma_{12} = (\sigma_{11} - \sigma_{22})/2\sigma_{12} \quad (2)$$

where  $J_e^0$  is the steady state shear compliance and  $\sigma_{ij}$  are the appropriate components of the stress tensor.

In most cases, researchers have considered a fully developed capillary flow, during which the energy is stored in the liquid. Following the emergence of the liquid from the orifice, the energy is released in a solid-like relaxation. As not all the swelling has to originate in such a mechanism, the elastic portion of  $B_{\text{exp}}$  will be written as  $B$  in the following text.

Spencer and Dillon<sup>1</sup> calculated  $DS$  from the solid-like recovery of shear stress as

$$s = B^2 - B^{-2}. \quad (3)$$

Nakajima and Shida<sup>2</sup> assumed that  $DS$  originated not in shear stress, but in normal stress difference in the capillary flow, and derived the following formula:

$$s = B^2 - B^{-4}. \quad (4)$$

Bagley and Duffey,<sup>3</sup> following the above analysis,<sup>2</sup> proposed the relation

$$s^2 = B^4 - B^{-2}. \quad (5)$$

Assuming that  $DS$  originates in the release of elastic energy stored in material during the flow through a capillary, Graessley et al.<sup>4</sup> calculated that

$$(J_e^0 \sigma_w^2 / 2G_s) \int_0^1 (\eta_0 \bar{r}^5 / \eta) d\bar{r} / \int_0^1 (\eta_0 \bar{r}^3 / \eta) dr = B^4 + 2/B^2 - 3 \quad (6)$$

where  $\sigma_w$ ,  $G_s$ , and  $\eta_0$  are the shear stress on the capillary wall, modulus of elasticity, and zero shear viscosity, respectively;  $\bar{r}^3 = r/R$  is the dimensionless radial position. From this equation, Bagley and Duffey<sup>3</sup> calculated

$$s^2 = B^4 + 2B^{-2} - 3 \quad (7)$$

and Vlachopoulos et al.<sup>5</sup>

$$s_w^2 = 3(B^4 + 2B^{-2} - 3). \quad (8)$$

In the last equation,  $s_w$ , called the "recoverable shear strain on the wall," is defined<sup>4</sup> as

$$s_w = J_e^0 \sigma_w. \quad (2a)$$

To be consistent, the "average" values of  $s$  used in eqs. (3)–(5) and (7) should be written as

$$s = J_e^0 \bar{\sigma}_{12} \quad (2b)$$

where  $\bar{\sigma}_{12}$  is the average value of shear stress across the capillary.

Using the concept of an average normal stress across the cross section of the extrudate and applying Henky's strain-elongation relation, Mendelson et al.<sup>6</sup> derived the formula

$$s^2 = 6B^2 \ln B. \quad (9)$$

It can be shown that, in the upper range of  $B$ , eqs. (5) and (9) are well approximated by the old, empirical relation<sup>7</sup>

$$s_w = 4(B - 1). \quad (10)$$

On the other hand, eq. (8) agrees rather well with the other empirical formula<sup>8</sup>

$$s_w = (B - 1)/0.155 \quad (11)$$

and the one derived by Cogswell,<sup>9</sup>

$$B^2 = (2s_w/3)[(1 + s_w^{-2})^{1/2} - s_w^{-2}]. \quad (12)$$

Much stronger dependence of  $s_w$  on  $B$  was predicted by Tanner<sup>10</sup> for the Poiseuille flow of KBKZ fluids:

$$s_w^2 = 2(B^6 - 1). \quad (13)$$

From the other relations between  $B$  and material parameters of the extrudate, the one proposed by Metzner et al.<sup>11,12</sup> based on momentum balance is worth mentioning. The relation was successful in predicting DS of polymer solutions<sup>11,12</sup> but failed for polystyrene melts.<sup>4</sup>

Before the relations between  $s$  and  $B$  are compared with the experimental results, it is important to reduce them to the same definitions and variables.

#### Relation Between the "Average" and "At the Wall" Recoverable Shear Strain

From eq. (6), using the power law approximation and comparing the result with eq. (7), the factor  $F$ , defined as

$$F = s/s_w \quad (14)$$

is found to depend on the power law exponent  $n$ :

$$F = \left[ \frac{3n + 1}{2(5n + 1)} \right]^{1/2}. \quad (14a)$$

The factor  $F$  can also be calculated directly from eqs. (2), assuming that the power law approximation also holds for the normal stress component:

$$(\sigma_{11} - \sigma_{22}) = K\dot{\gamma}^m. \quad (15)$$

After performing simple calculations,

$$F = 2n/(m + n) \quad (14b)$$

is found. This relation for small values of  $\dot{\gamma}$ , where  $J_e = J_e^0$  and  $m = 2n$  leads to  $F = 2/3$ ; whereas in the region of high rates of shear, where  $s$  is constant and  $m = n$ , it leads to  $F = 1$ .

### Definitions of $s$

In the derivation of eqs. (5) and (9), the authors<sup>3,6</sup> used Weissenberg's<sup>13</sup> definition of  $s$  as the ratio of the primary normal stress difference ( $\sigma_{11} - \sigma_{22}$ ) to the shear stress  $\sigma_{12}$ . However, the theoretical derivation of Lodge<sup>14</sup> indicated that  $s = (\sigma_{11} - \sigma_{12})/2\sigma_{12}$ . At the present time, this definition is generally accepted.<sup>15-17</sup> The Lodge definition was used in the other derivations of the  $s = s(B)$  relations quoted in this paper. Consequently, the values of  $s^2$  calculated from eqs. (5) and (9) should be divided by a factor of 2.

### Die Swell in the Newtonian Region

There are both experimental<sup>18,19</sup> and theoretical<sup>20-22</sup> indications that Newtonian liquids at low Reynolds number (Re) and viscoelastic liquids in the Newtonian range of  $\dot{\gamma}$  swell by 6.3-13.5%. This residual swelling is a consequence of the linearized Stokes equation<sup>21</sup> and is not significantly affected by inertia, surface tension, or residual viscoelasticity. The effect is kinematic in nature, and for this reason the elements near the axis, which suffer the greatest reduction in velocity at the exit must expand most.

On a purely empirical basis, Chapoy<sup>23</sup> separated  $B$  into dynamic and viscoelastic components, where the first amounted to 12% and 24-27% for polystyrene and polyethylenes, respectively.

The theoretical or semitheoretical relations  $s = s(B)$ , derived from consideration of the elastic swelling effect, should be compared with  $B_{\text{exp}}$  values from which the kinematic or residual contribution,  $B_0$ , has been subtracted:

$$B = B_{\text{exp}} - B_0. \quad (16)$$

Equation (16), which assumes an additivity of these effects,<sup>10,23</sup> seems to be preferable to the dependence

$$B = B_{\text{exp}}/(1 + B_0) \quad (16a)$$

used by Graessley et al.<sup>4</sup>

### Comparison Between the $s_w = s_w(B)$ Relations

A summary of the results computed from the afore-discussed relations between the recoverable shear strain and the die swell ratio  $B$  is presented in Figure 1. The values of  $s$  computed from eqs. (3)–(5), (7), and (9) were converted into  $s_w$  arbitrarily using  $F = 2/3$ . In addition, the results obtained from eqs. (5) and (9), based on Weissenberg's definition of  $s$ , were multiplied by  $2^{-1/2}$ .

In order to select one of these relations in the following calculations, the recoverable shear strain and the die swell parameter  $B$  of polystyrene sample PS-693 were measured over a wide range of  $\dot{\gamma}$ . For the details, see the experimental part. The results are presented in Figure 2. The recoverable shear strain values calculated from cone-and-plate rheometer data were converted to  $s_w$  by means of eq. (14b) in which the experimental values of both  $m$  and  $n$  were used. The broken circles were obtained by extrapolating the experimental  $(\sigma_{11} - \sigma_{22})$ -versus- $\dot{\gamma}$  dependence. It can be seen that the results follow eq. (13) rather well. The kinetic swelling parameter  $B_0$

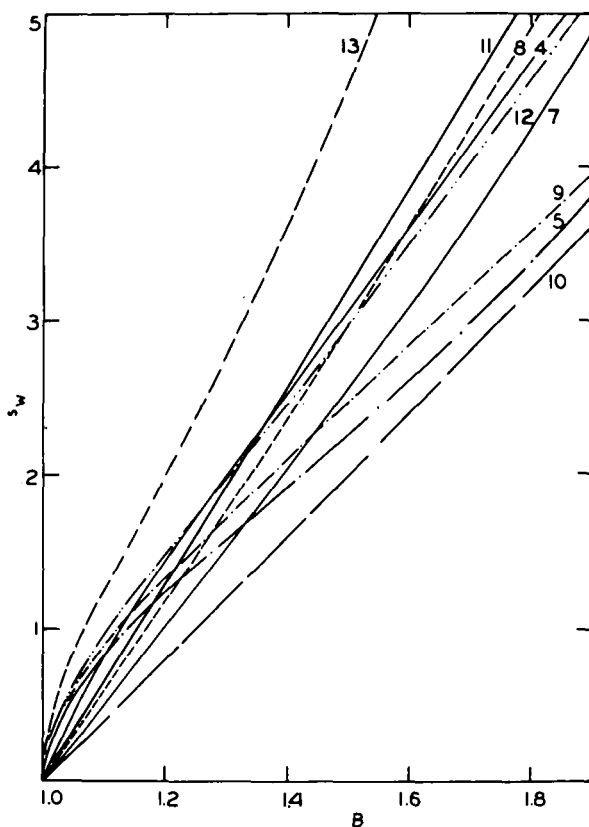


Fig. 1. Predicted dependence of shear strain on wall,  $s_w$ , on the elastic component of die swell,  $B$ . Numbers refer to the equations listed in text.

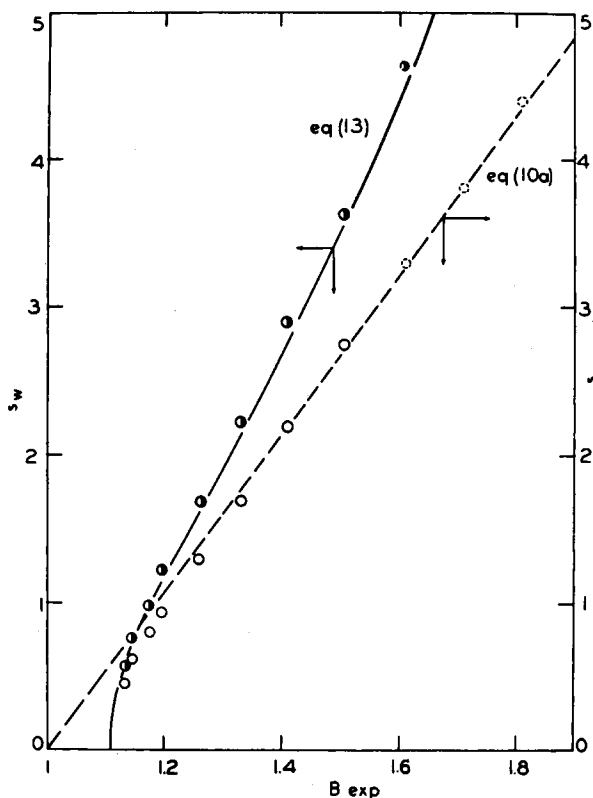


Fig. 2. Superposition of experimental dependences  $s_w$  vs.  $B_{exp}$  on the relation predicted by eq. (13). Broken line drawn through the open circles represents eq. (10a). Broken circles were calculated extrapolating the  $(\sigma_{11} - \sigma_{22})$ -vs.- $\dot{\gamma}$  curve to the appropriate rate of shear.

$= 0.11$  was found from the superposition of the theoretical curve. This value is smaller than 0.135 reported for Newtonian fluids,<sup>21,22</sup> but it is well within the range of values quoted for polymeric liquids.<sup>4,18,19</sup> In the same Figure 2, the values of  $s$  calculated directly from shear and normal stress data are plotted versus  $B_{exp}$ . It can be seen that for  $B_{exp} \geq 1.17$ ,  $s$  can be expressed by a very simple linear relation of the type used by Rigbi<sup>7</sup> and Spencer<sup>8</sup>:

$$s = a(B_{exp} - 1) \quad (10a)$$

with the numerical value of  $a = 5.3 \pm 0.1$ , falling in between the values quoted by these authors.

## EXPERIMENTAL

### Polymers

Five commercial polymers were used: two polystyrenes (PS), two polyethylenes (PE), and one poly(vinyl chloride) semirigid formulation

(PVC). The characteristic parameters of these samples are listed in Table I. The polymers were supplied by the manufacturers in a granular form. For the DS measurements, the samples were directly loaded to the rheometer barrel; for cone-and-plate rheometer tests, the samples were pressed into  $10 \times 10 \times 0.1$  cm sheets from which circular 2.5-cm-diameter specimens were cut out and repressed in a specially designed mold to fit the gap between the platens. The thermal stability of the PVC sample was tested both under static and dynamic conditions.<sup>24</sup> The rheological testing times were always shorter than the "time till discoloration."

### Rheological Testing

The polymers were tested in the Weissenberg rheogoniometer (WR) Model 18 equipped with 2.5 cm,  $4^\circ$  cone-and-plate arrangement in the steady shearing mode. Two torsion bars with the spring constants  $K_T = 877$  and 10,080 (dynes-cm/micron) were used. The normal force spring constant was  $K_N = 6,512$  (dynes/micron). The approximate range of rates of shear covered was  $\dot{\gamma} = 10^{-2}$ – $10^2$  ( $\text{sec}^{-1}$ ). The temperature of the platen was controlled by a commercial high-temperature chamber within  $\pm 2^\circ\text{C}$ ; the platen temperature was continuously recorded with the accuracy  $\pm 0.1^\circ\text{C}$ . The measurements yielded the rate of shear  $\dot{\gamma}$ , shear stress  $\sigma_{12}$ , and the primary normal stress difference  $\sigma_{11} - \sigma_{22}$  (dynes/cm<sup>2</sup>), wherefrom the viscosity  $\eta = \sigma_{12}/\dot{\gamma}$  (poise), primary normal stress difference  $\psi = (\sigma_{11} - \sigma_{22})/\dot{\gamma}^2$  (dynes-sec<sup>2</sup>/cm<sup>2</sup>), recoverable shear strain  $s = (\sigma_{11} - \sigma_{22})/2\sigma_{12}$ , and steady state compliance  $J_e = \psi/2\eta^2$  (cm<sup>2</sup>/dyne) were computed. The results were corrected for nonlinearity in transducer responses, shear heating, and centrifugal effects. For more details, see references 24–26.

In addition, the samples were tested using the Instron capillary rheometer (ICR) equipped with a capillary of length  $L = 5.14$  cm, diameter  $D = 0.127$  cm (i.e.,  $L/D = 40.5$ ), and  $90^\circ$  entrance angle. The shear stress on the wall was calculated by Sylvester's<sup>27</sup> method; the rate of shear on the wall was corrected<sup>28</sup> as usual.<sup>24</sup>

### Die Swell Measurements

Reliable die swell measurements have to be performed under the following conditions: (1) steady, isothermal flow; (2) absence of gravitational sagging and swelling due to interfacial tension; (3) the extrudate should be in a state of complete elastic recovery.

There are two main methods of die swell measurements. In the first, the extrudate is quenched in air or liquid; in the second, the polymer is extruded into a heated chamber and relaxed, and then the dimensions are measured. The simplest technique is to measure the diameter of an extrudate  $1/4$  in. above its free end as employed by a number of workers.<sup>5,29,30</sup> Nakajima and Shida<sup>2</sup> obtained measurements by relaxing 1.5-in.-long strands of extrudate suspended in an oven and recording the diameter changes of film. Mendelson et al.<sup>6</sup> relaxed such strands in an oil bath and measured the diameter of a cold sample with a micrometer. It has been

TABLE I  
Characteristic Parameters of the Polymers

No.	Code	Polymer	Manufacturer	$M_n \times 10^{-3}$	$M_w \times 10^{-3}$	$M_{st,1}/M_n$	Comments
1	PVC	poly(vinyl chloride)	B. F. Goodrich	0.834	1.72	3.99	69.9 wt-% PVC, 25.2 plasticizer, 4.9% lead stabilizer, see reference 24.
2	PE-58	polyethylene	du Pont	0.273	2.04	---	density $\rho = 0.9619$ , melt index $MI = 0.44$ , 1.5% $\alpha$ -olefins added
3	PE-59	polyethylene	du Pont	0.277	1.85	---	$\rho = 0.9561$ , $MI = 0.42$ , homopolymer
4	PS-693	polystyrene	Dow Chemical	0.95	2.65		
5	PS-678	polystyrene	Dow Chemical	1.05	2.42		



demonstrated that the final diameter of the extrudate does not depend on the temperature of relaxation. Cogswell<sup>9</sup> quenched the rod or disk shaped extrudates in cold water. Later, the samples were allowed to relax in a hot oven. Extrusion into a heated gas chamber was described by Petraglia et al.<sup>31</sup> and Han and co-workers.<sup>32,33</sup> However, neither of the two methods, quenching or extruding into a hot chamber, provides the three conditions necessary for reliable measurements of DS. Quenching introduces an additional thermal history, which in the case of crystallizable polymers introduces additional stresses.<sup>6</sup> Extrusion into a hot gas chamber increases the effect of gravitational sagging and interfacial tension.

Extrusion of polymer into an inert thermostated fluid of proper density and interfacial tension seems to satisfy all three basic conditions. This method was recognized and used before to study DS of polystyrenes.<sup>4</sup> For this polymer, a small difference was found between DS measured by extruding into a thermostated bath and quenched in the air.

### Semiautomatic DS Measurements

An effort was made to design a system which would allow fast and precise measurements of true DS. Figure 3 shows a block diagram of the system. The liquid into which the samples are extruded is maintained at constant temperature by employing a Neslab thermostat (1) equipped with an additional 750-W quartz heater with a variable transformer. The liquid flows through a manual valve (2), flexible hose (3), and solenoid valve (4) to the bottom of the thermostating chamber (5), from where it returns under

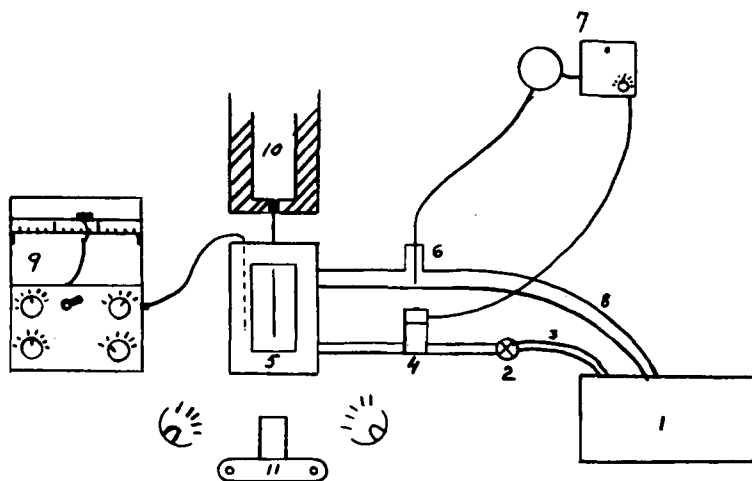


Fig. 3. Block diagram of arrangement used to measure die swell: (1) thermostating circulating bath; (2) manual valve; (3) stainless steel flexible inlet hose; (4) solenoid valve; (5) thermostating chamber; (6) T-joint pipe fitting for sensor of the liquid level controller; (7) oscillator relay for liquid level controller; (8) stainless steel flexible outlet hose; (9) Azar thermocouple recorder; (10) Instron capillary rheometer; (11) camera

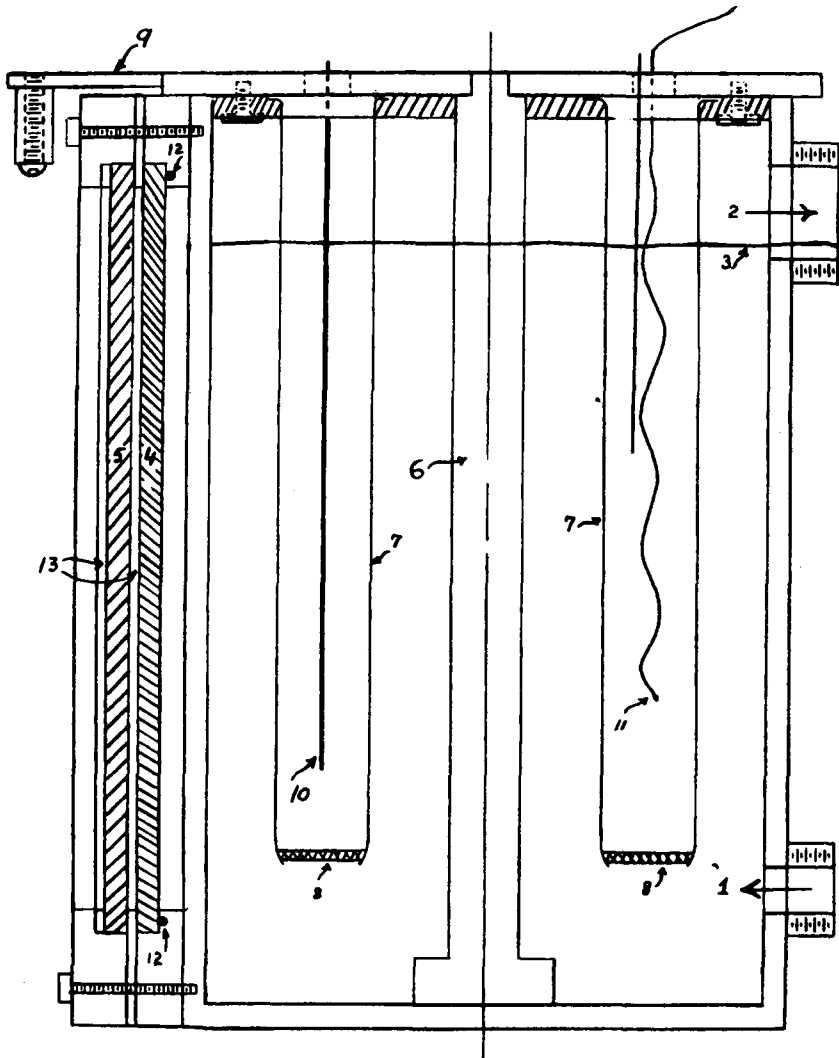


Fig. 4. Cross-sectional view of thermostating chamber: (1) liquid inlet; (2) outlet fittings; (3) liquid level; (4) Vycor; (5) Pyrex glass plates; (6) central shaft; (7) Pyrex glass tubes; (8) stainless steel screens; (9) shears; (10) polymer extrudate; (11) thermocouple wire and calibration rod; (12) Viton-O-Ring; (13) asbestos sheet.

gravity to (1) through a T-pipe (6) (equipped with a liquid level controller (7)) and a flexible hose (8). The temperature of the liquid is continuously monitored by a thermocouple placed in one of the thermostating chamber sample holders and recorded on (9). The polymer is extruded from a capillary rheometer (10) to the thermostating chamber (5). A single-lens reflex camera (11) is used to record the changes of the extrudate diameter with time.

The thermostating chamber was rigidly connected to a cart housing the NesLab thermostat and to a camera. In this manner, the whole assembly could be pushed in to collect the extrudate, photograph the initial stage of the DS, and then to pull out and continue the DS measurements while the rheometer was being prepared for the next extrusion, or cleaned.

A schematic diagram of the thermostating chamber is shown in Figure 4. The chamber is made of a piece of stainless steel pipe, ID = 6 in., length = 10 in., to which the bottom plate, inlet (1) (ID =  $\frac{1}{2}$  in.) and outlet (2) (ID = 1 in.) connectors and the central shaft (6) are welded. One side of the pipe has been cut off and in this space a flange is welded on which a double window (a sandwich of Viton ring, Vycor glass, asbestos plate, Pyrex glass, and asbestos plate) is mounted. The cover rotating on the central shaft is made of an H-M marinite (compressed asbestos fibres and diatomaceous silica)  $\frac{3}{4}$ -in. board fixed to a  $\frac{1}{8}$ -in. stainless steel plate. The cover has six holes, ID =  $\frac{1}{2}$  in. In these holes, six glass tubes (7), equipped with a stainless steel mesh (8) at the bottom, are suspended. Each of the holes is provided with dual action shears (9) which cut off the sample (10) and hold it in a fixed position. The monitoring thermocouple (11) is placed in one of the tubes. It was found that equally good results could be obtained by replacing the open bottom glass tubes with closed bottom ones, filled with a liquid other than that used to thermostat the system. This was particularly valuable in the case of DS measurements of PVC, for which an expensive fluorosilicone oil was used.

The details of the cover plate of the thermostating chamber are shown in Figure 5. Here, the arrangement for six tubes is shown. Four of these are used to collect the extrudate, one contains a size calibration plate, and one holds the thermocouple. If necessary, more or less holes can be used, without substantial change of the design.

### Procedure for the Measurement of Die Swell

It is of basic importance to properly select the swelling temperature ( $TB$ ).  $TB$  has to be above any phase transition of the polymer but below its degradation temperature. The polymer at  $TB$  should have high enough viscosity so that the flow within the extrudate volume under the small gravitational pull:  $(\rho_P - \rho_L)g/L$  can be neglected. (Here,  $\rho_P$  and  $\rho_L$  are the densities of the polymer and thermostating liquid, respectively;  $g$  is the gravitational constant; and  $L$  is the length of the extrudate hanging below the level of measurement of extrudate diameter.) Furthermore, the thermostating liquid should be inexpensive, thermally stable up to  $TB$ ; should have  $\rho_L \approx \rho_P - 0.1$ , in g/cc; should not swell or dissolve the polymer; and the interfacial tension between the liquid and extrudate should be nearly zero. A list of the thermostating liquids used in this work is given in Table II.

For the studies reported in this paper, the Instron capillary rheometer (ICR) was used. The rheometer barrel was raised by 20 cm, and two Thomson Ball rails were fixed to the ICR table. However, the chamber

TABLE II  
Thermostating Liquids Used in DS Experiments

Polymer	Liquid	No.*	<i>T<sub>B</sub></i> , °C	Viscosity at 25°C	Density at 23°C, g/ml	Flash point, °C
Poly(vinyl chloride)	fluorosilicone fluid	FS1265	160	10 st.	1.28	290
Polyethylene	silicone fluid	200	155	5 c st.	0.92	135
Polystyrene	silicone fluid, 78 wt-%, + 22% di( <i>n</i> -octyl) phthalate	200	150	2 st.	0.971	315

\* Dow Corning Silicone Fluids.

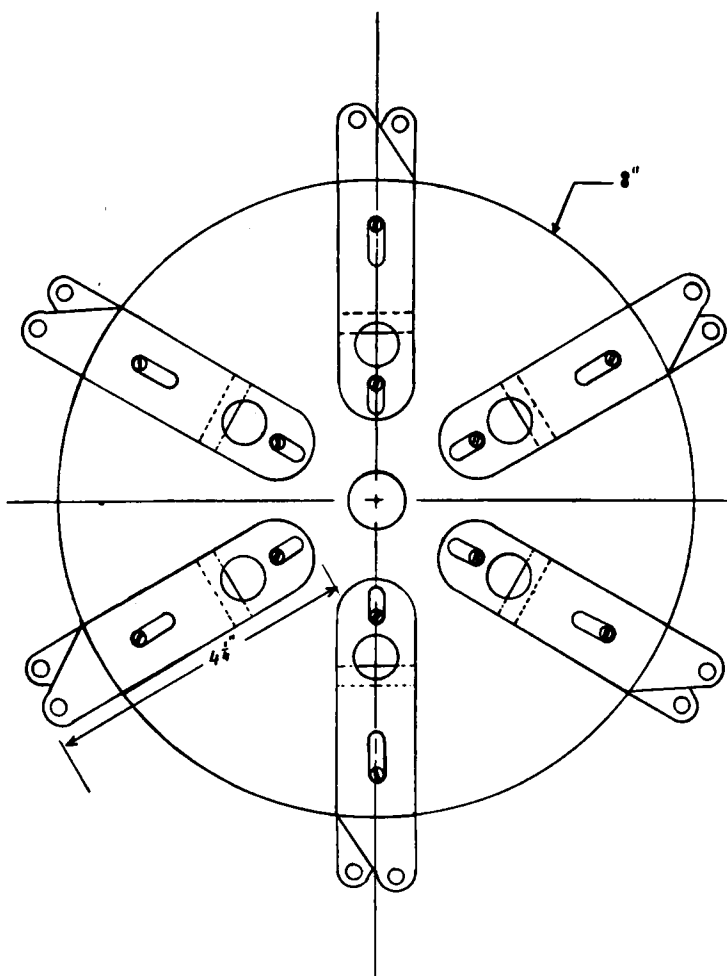


Fig. 5. Top plate of thermostating chamber equipped with six pairs of shears to cut off and to hold the polymer extrudate.

TABLE III  
Sequence of Cross-Head Speeds<sup>a</sup>

No.	Run: 1			Run: 2			Run: 3			Run: 4		
	<i>V</i>	<i>G</i>	<i>t</i>	<i>V</i>	<i>G</i>	<i>t</i>	<i>V</i>	<i>G</i>	<i>t</i>	<i>V</i>	<i>G</i>	<i>t</i>
1	0.5	20	2.0	0.2	20	2.0	0.1	20	2.0	0.05	20	4
2	1.0	19	5.0	2.0	19.6	3.0	5.0	19.8	1.0	5.0	19.8	1
3	10.0	14	1.0	20.0	13.6	0.5	20.0	14.8	0.5	50.0	14.8	0.29
4	2.0	4	2.0	1.0	3.5	3.6	0.5	4.8	6	—	0	—
	—	0	—	—	0	—	—	1.8	—			
Total time:			10			9.1			9.5			5.29

<sup>a</sup> *V* = Cross-head velocity (cm/min); *G* = gauge reading (cm); *t* = extrusion time (min).

and the proposed method of DS measurements can be adapted to any capillary rheometer.

In order to accelerate the initial heating up of the system, the additional heater in the thermostat was utilized. When the temperature recorded by the thermocouple (no. 11 in Fig. 2) reached a stable  $T = TB$  level (ca. 2 hr), the rheometer was loaded with the polymer (ca. 6 min), the Instron load cell was calibrated (2 min), and a small amount of the polymer extruded, so that the starting level of the cross head was always the same. The measurements, starting 10 min after the beginning of the loading of the rheometer, followed one of the four sequences quoted in Table III. Next, the thermostating chamber was pushed in, aligned with the die exit, and the first sample collected and photographed. Excepting the lowest rates of extrusion ( $V \leq 0.05$  cm/min), ca. 15-cm-long strands were used. The six first photographs were taken within 1 min after the shears (see Fig. 5) were snapped. The strand were photographed for 40 min of swelling time. The extrudates used for DS measurements were collected in the time interval when the recorded pressure indicated steady state flow. After the four samples were collected in the thermostating chamber, the rheometer was cleaned and prepared for the next run while the strands were photographed in the desired sequence and time intervals.

The developed film was analyzed using a Nikon Shadowgraph Model 2. The diameter of the extrudate was measured 2 and 5 cm above its lower end within  $\pm 0.01$  mm. The actual diameter was calculated knowing the true dimension of the size calibration plate, photographed in the beginning and in the end of each roll of film.

The addition of the DS measurements increased the operating time of ICR by 30%, in respect to the standard viscosity determination time. However, the design of the apparatus allowed the standard measurements of viscosity on ICR to be obtained without interference.

## RESULTS

In Figure 6, an example of the time dependence of extrudate diameter  $D$  is shown. In all cases, the dependence can be divided into three regions:

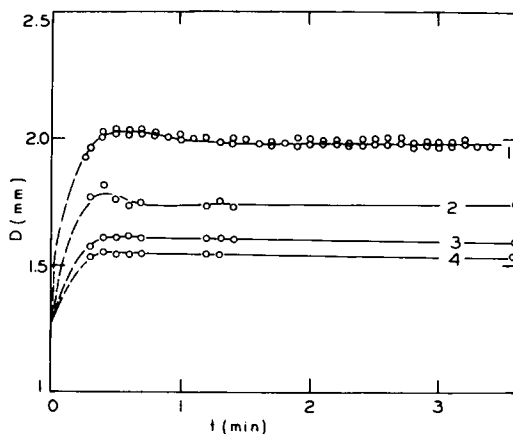


Fig. 6. Time dependence of the extrudate diameter of PS-693. Extrusion temperature, 190°C; thermostating liquid temperature, 125°C. Numbers refer to rates of shear:  $\log \dot{\gamma} = 2.96, 2.26, 1.96,$  and  $1.66$  for 1–4, respectively.

(a) rapid swelling, (b) shrinkage due to difference in temperature between the ICR and the thermostating liquid, and (c) the equilibrium region. It can be demonstrated that the actual swelling time should be short. It is customary<sup>34</sup> to consider  $40 \times$  relaxation time as a period sufficient for the elastic recovery. Since the relaxation times for the extruded polymers is  $\tau_0 < 1$  sec, the expected relaxation times should be less than 40 sec. Simultaneously with the swelling, shrinkage (process (b)) takes place. For the system presented in Figure 6, it can be calculated<sup>35</sup> that the time required for the center of the extrudate to reach 127°C (here  $TB = 125^\circ$ , barrel temperature  $T = 190^\circ\text{C}$ ) is 22–30 sec. Furthermore, the magnitude of the decrease of  $D$  with time is consistent with the values calculated from the thermal expansion coefficient.<sup>36</sup> The region (c) was found to extend up to 90 min, provided the densities, interfacial tension, and  $TB$  were properly selected; e.g., for PVC ( $T = 200$ ,  $TB = 186$ ,  $\rho_P - \rho_L = 0.4$ , a flow of the extrudate was observed due to the large density gradient and the relatively low polymer viscosity. The  $B_{\text{exp}}$  values quoted in the following text were determined from the equilibrium data (region (c)), using the appropriate<sup>36</sup> thermal expansion coefficient to correct for the difference of the temperature between the rheometer and the thermostating chamber, i.e., all the  $B_{\text{exp}}$  discussed in this paper are the equilibrium swelling ratios at the extrusion temperature.

The experimental results of DS measurements are presented in Figure 7 as  $B_{\text{exp}}$ -versus- $\dot{\gamma}$  plot. It is worth noting that the swelling of both polystyrene samples follows the same dependence in spite of the difference in their viscous behavior: By contrast, the two polyethylenes show a remarkable difference in DS, whereas their  $\eta$ -versus- $\dot{\gamma}$  dependences do not differ much. The die swell behavior of the PVC compound indicates an unusual pattern, passing through a shallow minimum. The low values of  $B_{\text{exp}}$

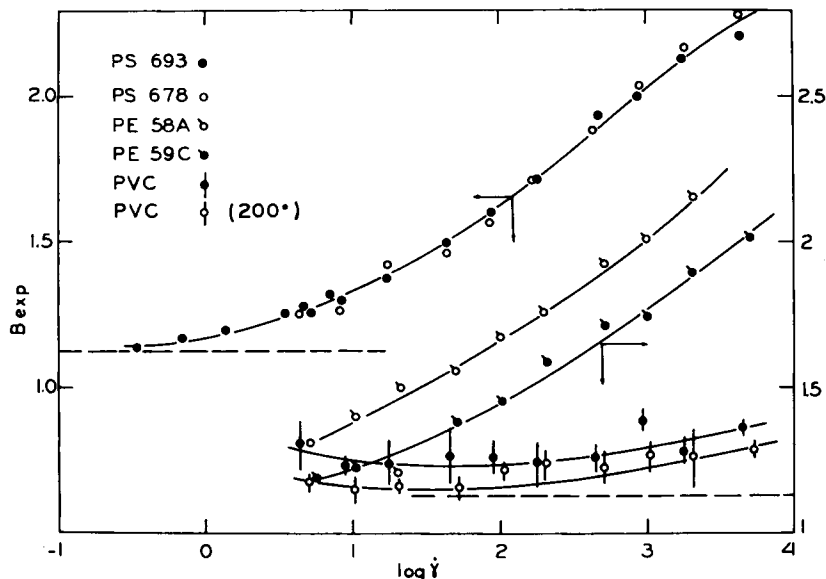


Fig. 7. Shear dependence of swelling ratio  $B_{exp}$  for indicated polymers. The extrusion temperature for all but the last (PVC = 200°C) sample was 190°C. The  $B_{exp}$  for PE and PVC are vertically displaced by 0.5 in respect to PS values.

observed for this polymer indicate small stored energy of flow. Here, the increase of temperature decreases the DS.

In Figures 8-13, the rate of shear dependences of  $\eta$  and  $d$  are shown for each of the studied systems. The details of  $\eta$ -versus- $\dot{\gamma}$  calculations were given before.<sup>24-26</sup> The solid lines which approximate this dependence were computed<sup>26</sup> from the Graessley et al.<sup>37</sup> theory. The values of  $s$  from WR were computed using Lodge's definition of  $s$ , and those from ICR were computed from  $B_{exp}$  using eq. (13). In these calculations,  $B_0 = 0.11$  was assumed for all polymers. The conversion factor  $F$  was computed from eq. (14b), knowing the values of  $m$  and  $n$  from WR results. The solid lines which are drawn through the  $s$ -versus- $\dot{\gamma}$  data points are arbitrary.

## DISCUSSION

The proposed new chamber and the procedure of DS measurements will be discussed first. The method is inexpensive both in material and operating costs. It leads to reliable, reproducible results; it can be used for various materials by varying the type and the temperature of the thermostating fluid. Furthermore, by changing from the photographic to the laser beam method of diameter recording, it can be made semiautomatic, increasing both speed and accuracy of the measurements. The chief advantage of the method is that, for the first time, DS of semicrystalline polymers (like PE) can be measured immediately, without introducing an extra stress-thermal history to the sample. The disadvantages of the

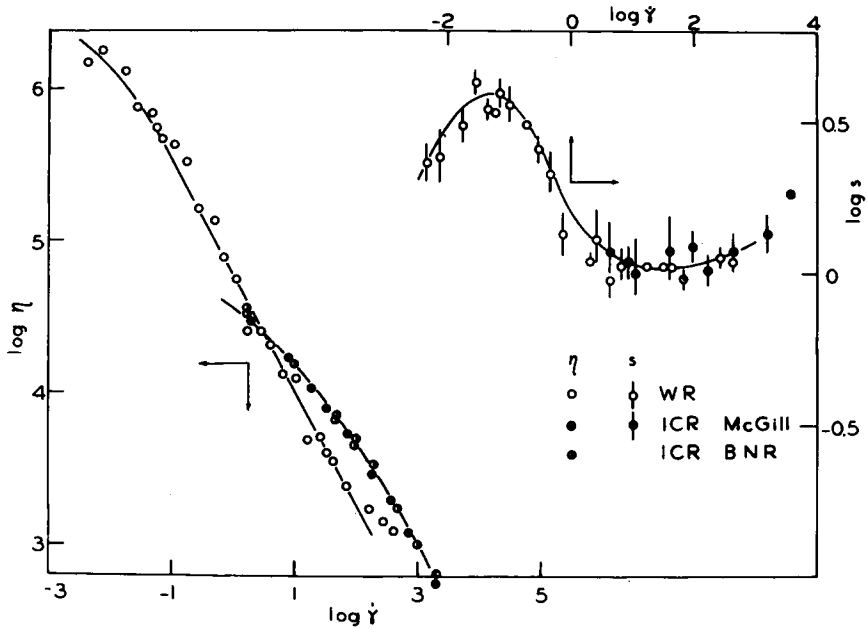


Fig. 8. Shear rate dependence of viscosity  $\eta$  and recoverable shear strain  $s$  for PVC extruded at 190°C. Open circles represent the WR data; filled and half-filled circles, the ICR results.

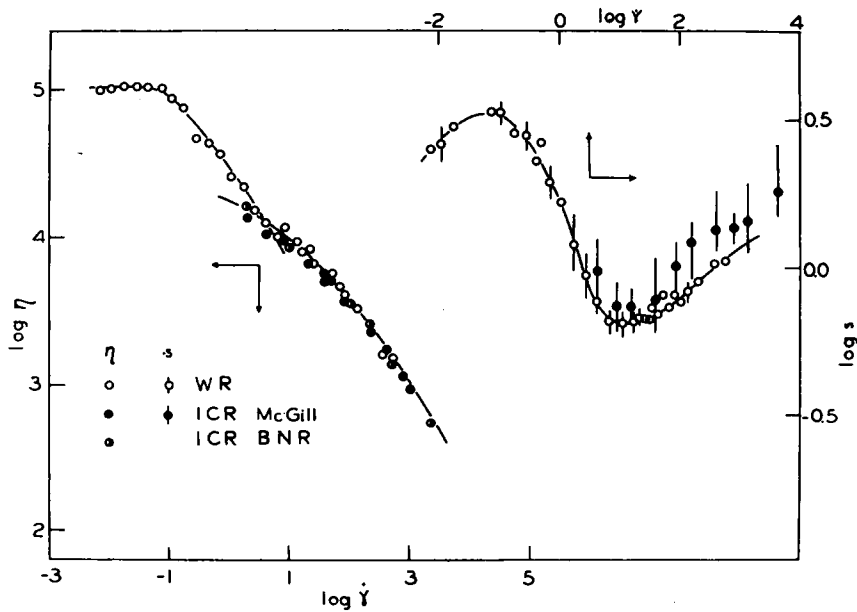


Fig. 9. Shear rate dependence of viscosity  $\eta$  and recoverable shear strain  $s$  for PVC extruded at 200°C. Open circles represent the WR data; filled and half-filled circles, the ICR results.



method are: difficulty in collecting the extrudate at the highest and at the lowest rates of extrusion, difficulty in selecting the proper fluid for the given material, and the bulkiness of the thermostat plus thermostating chamber assembly.

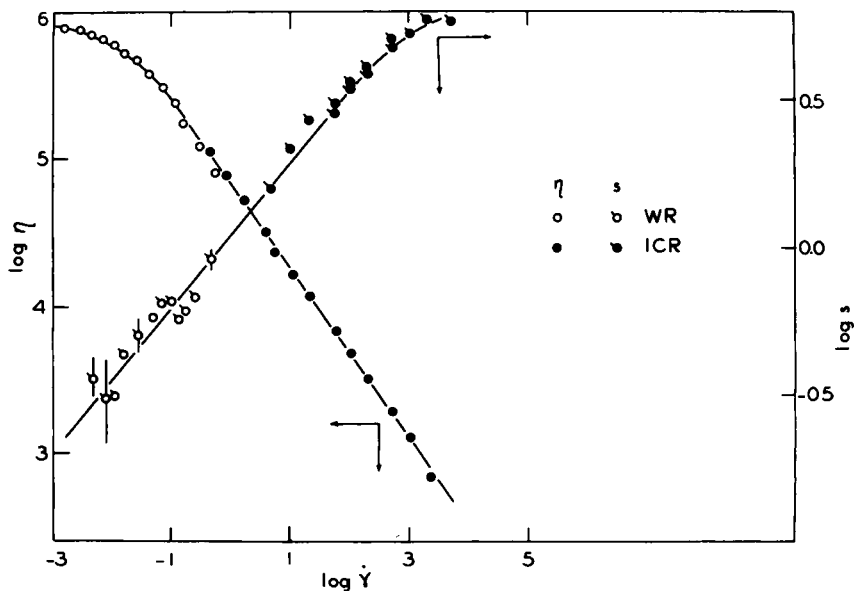


Fig. 10. Shear rate dependence of  $\eta$  and  $s$  for PE-58 at 190°C. Open and filled circles represent the WR and ICR results, respectively.

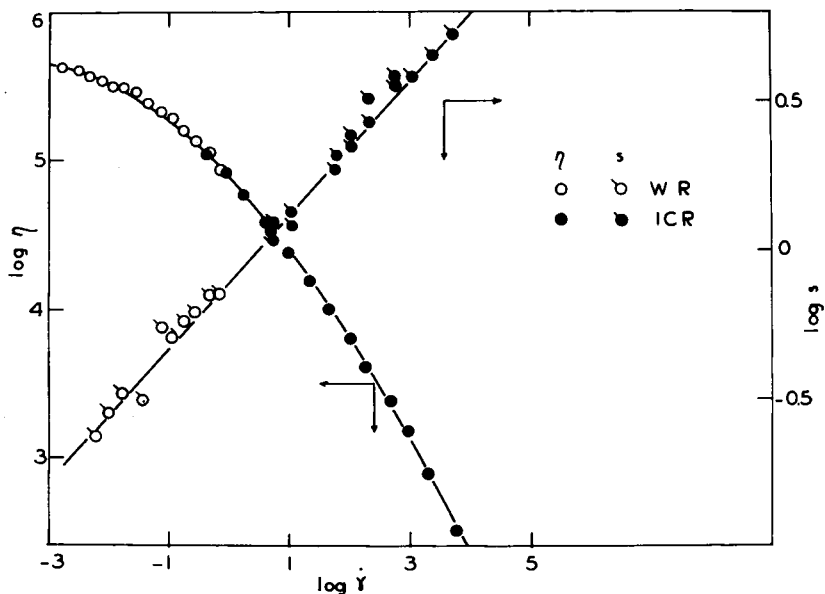


Fig. 11. Shear rate dependence of  $\eta$  and  $s$  for PE-59 at 190°C. Open and filled circles represent the WR and ICR results, respectively.

All the DS experiments presented in this paper were performed using a single capillary with  $L/D = 40.5$ , assuming that the results are independent of the capillary geometry. This assumption should be valid for PS,<sup>4,5</sup> but it may not be so for PE—there are controversial reports regarding this

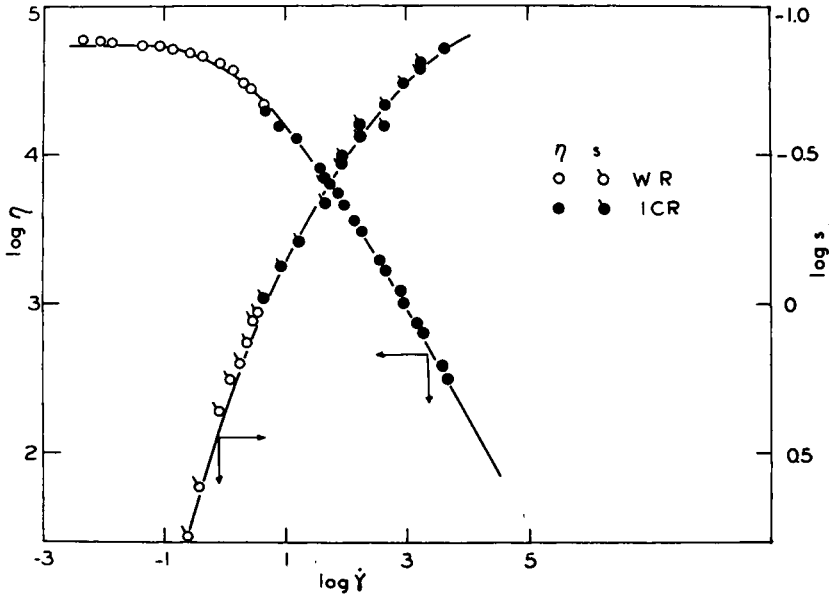


Fig. 12. Shear rate dependence of  $\eta$  and  $s$  for PS-678 at 190°C. Open and filled circles represent the WR and ICR results, respectively.

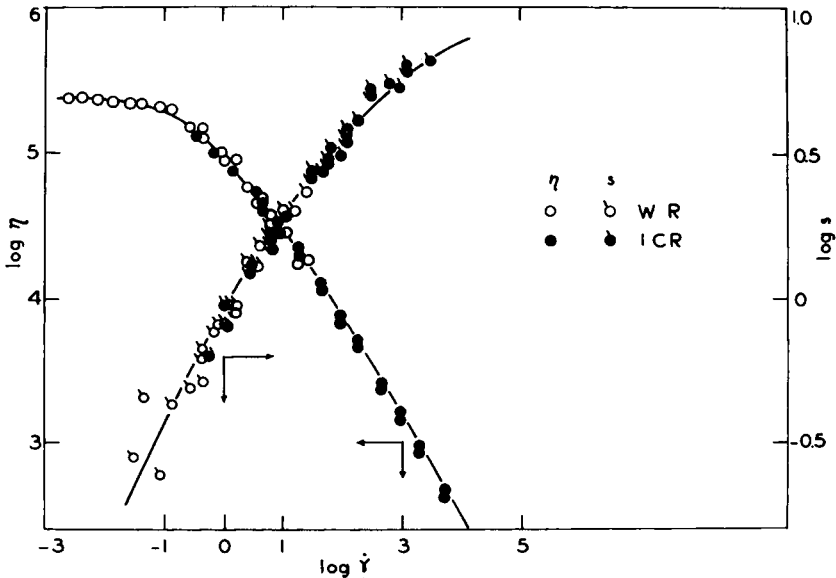


Fig. 13. Shear rate dependence of  $\eta$  and  $s$  for PS-693 at 190°C. Open and filled circles represent the WR and ICR results, respectively.

polymer which can be used either to prove<sup>2,6</sup> or disprove<sup>30,38,39</sup> the validity of this assumption. The capillary flow of PVC formulations can be nonviscometric,<sup>24</sup> and, for this reason, the dependence of  $B_{\text{exp}}$  on  $L/D$  ratio should be tested for each new compound. This has not been done for the formulation under study. If the swelling of PE and PVC samples did not reach its equilibrium value at  $L/D = 40.5$ ; then the reported values of  $B_{\text{exp}}$  can be larger than expected. However, the  $B_{\text{exp}}$ 's (see Fig. 7) of PVC at 190° and 200°C are only slightly larger than those reported<sup>18,19,22</sup> for Newtonian liquids, whereas  $B_{\text{exp}}$  values of PE-58 are systematically lower by approximately 0.5 units than those reported<sup>6</sup> for a similar resin.

Tanner's<sup>10</sup> eq. (13), used in this work to compute  $s$  from  $B_{\text{exp}}$ , is based on KBKZ fluid model<sup>40,41</sup> with an additional assumption that  $s \propto \sigma_{12}$ . This assumption is strictly valid in the range of low rates of shear at the onset of non-Newtonian behavior and in terms of the power law exponents is equivalent to the following conditions:  $m = 2n$  or  $F = 2/3$ . These equalities are valid only over limited range of  $\dot{\gamma}$  for the systems studied. However, it can be shown that if a more general assumption was used in Tanner's derivation, namely  $s \propto \sigma_{12}^b$ , where  $b \leq 1$ , the factor of 2 in eq. (13) would have to be substituted by  $(b^2 + 1)$ ; and, as a result, the quoted values of  $s_w$  would have to be multiplied by a factor of

$$0.707 \leq [(b^2 + 1)/2]^{1/2} \leq 1.0.$$

This means that the log  $s$  data points in Figures 8–13 can be too large by less than 0.15 unit at the highest rates of shear.

The results of computation of  $s$  from DS for PS and PE samples show a remarkable agreement with the values calculated from the WR results. The agreement for PS-693 is forced by selecting Tanner's relation as the only one which follows the observed dependence. However, it can be seen that for the remaining three samples, the two sets of  $s$  values either overlap or coincide in the intermediate range of  $\dot{\gamma}$ .

The relatively good agreement between the two sets of  $s$  values shown in Figures 8 and 9 for PVC compound was not expected. It was demonstrated<sup>24–26</sup> that PVC formulations, below the melting temperature of the lamellar structure, flow through a capillary by a plug flow (skin-and-core) mechanism. This results in a difference between the flow curves determined in WR and ICR, as visible in Figure 8. Furthermore, the low values of DS indicate that a particulate mechanism of flow is to be expected. If so, the molecular entanglements necessary for generation of normal stresses must take place either in the skin or interparticle region or in both of these. The agreement between values of  $s$  determined on the basis of WR normal stress measurements and those calculated from experimental DS values may suggest that the interparticle regions in the central plug participate in the swelling of the extrudate.

The results presented in this report support the earlier observations of Tanner<sup>10</sup> and Vlachopoulos et al.<sup>5,42</sup> It may be of interest to note that the values of  $s$  calculated from the empirical formula (10a) fall in between those predicted by the two other empirical dependencies, eqns. (10) and (11). It

can be demonstrated that the magnitude of the parameter  $a$  in eq. (10a) will depend on the numerical value of the power law parameters  $n$  and  $m$ .

The authors are indebted to Drs. Y. Kuo and J. M. Dealy of this University for valuable discussions. The criticisms of Mrs. M. Farago, Northern Electric Co., and Dr. C. Elston, Du Pont of Canada, are deeply appreciated. This work was supported by National Research Council of Canada Grant PRAI S-20.

### References

1. R. S. Spencer and R. E. Dillon, *J. Colloid Sci.*, **3**, 163 (1948).
2. N. Nakajima and M. Shida, *Trans. Soc. Rheol.*, **10**, 299 (1966).
3. E. B. Bagley and H. J. Duffey, *Trans. Soc. Rheol.*, **14**, 545 (1970).
4. W. W. Graessley, S. D. Glasscock, and R. L. Crowley, *Trans. Soc. Rheol.*, **14**, 519 (1970).
5. J. Vlachopoulos, M. Horie, and S. Lidorikis, *Trans. Soc. Rheol.*, **16**, 669 (1972).
6. R. A. Mendelson, F. L. Finger, and E. B. Bagley, *J. Polym. Sci. C*, **35**, 177 (1971).
7. Z. Rigbi, *SPE J.*, **22** (Sept. 1953).
8. R. S. Spencer, in *Physics of Plastics*, P. D. Ritchie, Ed., Butterworth, London, 1965.
9. F. N. Cogswell, *Plastics and Polymers*, 391 (December 1970).
10. R. I. Tanner, *J. Polym. Sci. A-2*, **8**, 2067 (1970).
11. A. B. Metzner, W. T. Houghton, R. A. Sailor, and J. L. White, *Trans. Soc. Rheol.*, **5**, 133 (1961).
12. R. F. Ginn and A. B. Metzner, in *Proc. 4th Int. Congress of Rheology*, Part 2, E. H. Lee, Ed., Wiley, New York, 1965.
13. K. Weissenberg, *Proc. 1st Int. Congress on Rheology*, **1**, 29 (1948). Amsterdam, 1949.
14. A. S. Lodge, *Trans. Faraday Soc.*, **52**, 120 (1956).
15. J. D. Ferry, *Viscoelastic Properties of Polymers*, Wiley, New York, 1970.
16. R. A. Stratton and A. F. Butcher, *J. Polym. Sci. A-2*, **9**, 1703 (1971).
17. B. D. Coleman and H. Morkovitz, *J. Appl. Phys.*, **35**, 1 (1964).
18. S. Middleman and J. Gavis, *Phys. Fluids*, **4**, 355 (1961).
19. J. Gavis and M. Modan, *Phys. Fluids*, **10**, 487 (1967).
20. S. Richardson, *Rheol. Acta*, **9**, A193 (1970).
21. R. I. Tanner, paper presented at the US-Japan Joint Seminar on Polymer Processing, Knoxville, Tennessee, 1972.
22. F. Horsfall, *Polymer*, **14**, 262 (1973); J. Batchelor, J. P. Berry, and F. Horsfall, *ibid.*, 297 (1973).
23. L. L. Chapoy, *Rheol. Acta*, **8**, 497 (1969).
24. L. A. Utracki, Z. Bakerdjian, and M. R. Kamal, paper presented at the 1973 Annual Meeting of Society of Rheology in Montreal. *Trans. Soc. Rheol.*, to be published.
25. L. A. Utracki, *SPE Technical Papers*, **19**, 567 (1973); *Polym. Eng. Sci.*, **14**, 308 (1974).
26. L. A. Utracki, *J. Polym. Sci., Polym. Phys. Ed.*, **12**, 563 (1974).
27. N. D. Sylvester, *J. Macromol. Sci.*, **A3**, 1033 (1969).
28. B. Rabinovitch, *Z. Phys. Chem.*, **A145**, 1 (1929).
29. T. Arai and H. Aoyama, 33rd Annual Meeting of the Society of Rheology, Baltimore, 1962; *Trans. Soc. Rheol.*, **7**, 333 (1963).
30. M. G. Rogers and C. McLuckie, *J. Appl. Polym. Sci.*, **13**, 1049 (1969); *ibid.*, **14**, 1679 (1970).
31. G. Petraglia and A. Coen, *Polym. Eng. Sci.*, **10**, 79 (1970).
32. C. D. Han and M. Charles, *Trans. Soc. Rheol.*, **14**, 213 (1970).
33. C. D. Han and T. C. Yu, *A.I.Ch.E. J.*, **17**, 1512 (1971).
34. e.g. see W. T. Laughlin, and D. R. Uhlmann, *J. Phys. Chem.*, **76**, 2317 (1972).
35. A. J. Chapman, *Heat Transfer*, 2nd ed. MacMillan, Toronto, 1967, p. 135.

36. J. Brandrup and E. H. Immergut Eds., *Polymer Handbook*, Interscience, New York, 1966.
37. W. W. Graessley and L. Segal, *Macromolecules*, **2**, 49 (1969).
38. E. B. Bagley, S. H. Storey, and D. C. West, *J. Appl. Polym. Sci.*, **1**, 1661 (1963).
39. A. P. Metzger and J. D. Matlack, *Polym. Eng. Sci.*, **8**, 110 (1968).
40. A. Kaye, Coll. Aeronautics, Cranfield, Notes No. 134, 1962.
41. B. Bernstein, E. Kearsley, and L. Zapas, *Trans. Soc. Rheol.*, **7**, 391 (1963).
42. J. Vlachopoulos, paper presented at the VIth International Congress in Rheology, Lyon, 1972; *Rheol. Acta.*, **13**, 223 (1974).

Received June 20, 1974

Revised August 5, 1974